Nanoscale measurements for computing Young's modulus with atomic force microscope

A. D. Kaul, A. Gangwal* and S. S. Wadhwa†

Central Scientific Instruments Organization, Sector 30, Chandigarh 160 020, India
*Birla Institute of Technology and Science, Pilani 333 031, India

Atomic force microscope (AFM), developed at Central Scientific Instruments Organization, Chandigarh, has been configured for load–depth indentation measurements, wherein 'the reverse path effect' of AFM force curve associated with the use of piezo actuators has been overcome by measuring *in situ* actuator displacement independently by a laser Doppler displacement meter (LDDM) to enable correction of the force curves. The measurements of elastic moduli of highly oriented pyrolytic graphite, silicone elastomer, mica and gallium arsenide have been carried out.

THE force between the tip mounted on a cantilever beam and the sample surface as a function of the tip-surface separation can be computed with an atomic force microscope (AFM)[1]. The nanomechanical properties of the sample originating from the force associated with the tip–surface interaction have been studied by the AFM developed at Central Scientific Instruments Organization, Chandigarh[2].

Determining the mechanical properties of materials on nanometer scale, as desired in semiconductor industries and microsystems, requires special instruments having high lateral and depth resolution. This has been pursued by the nanomechanics and AFM communities[3]. In typical nanoindentation studies, the penetration of the indenter tip into the sample is measured as a function of applied load. AFM when used in an indentation mode, can measure the mechanical properties of surfaces with unprecedented force and lateral/penetration–depth resolution[4].

These AFM measurements are significantly affected both with regard to indentation curve shape and quantitative values of measurement by well-known effects of hysteresis and creep in lead zirconate titnate (PZT) piezo actuators used to control the positioning and motion of the mechanical components (cantilever, tip, etc.) of the AFM. An ideal behaviour is usually assumed for these actuators in which a reproducible displacement results for a given applied voltage, regardless of the magnitude of the voltage or the recent translation history of the actuator. Both these factors affect the response of the piezoelectric actuator, and the measured force curve is distorted when the tip is retracted from the sample. The unloading portion of the curve yields a higher applied load than the loading portion. This phenomenon called 'reverse path effect' is an instrumental artifact[5]. These adverse effects limit the use of AFM for quantitative measurements.

The problem could be overcome by removing the piezoelectric actuators[5] or by measuring displacement of the PZT actuator independently. In this study, the displacement has been measured optically by laser Doppler displacement meter (LDDM)[6] showing a measurement accuracy of one part per million. This electro-optical device detects the Doppler shift of a laser frequency caused by a moving target. The voltage–displacement plots of piezo actuator were obtained and corrections to the force curves were thus made.

The measurement of elastic moduli of highly oriented pyrolytic graphite (HOPG), silicone elastomer, mica and gallium arsenide (GaAs) have been carried out and presented in this paper.

Basically, a force microscope is comprised of a sensor (tip mounted on a cantilever which deflects due to force interaction between the sample and the tip) and a detector. The detector measures the cantilever position which is used to determine the force (F) on the tip using Hook's law i.e. $F = KZ$, where K is the stiffness of the cantilever and Z is the cantilever displacement.

Instrumental details of AFM configured for this work are shown in Figure 1, wherein 'A' shows the optical deflection system consisting of a laser diode, focussing optics, cantilever with its mount, and the position sensitive detector (PSD) to measure the deflection of the cantilever. AFM stage consisting of magnetic sample holder, differential micrometer operated coarse approach mechanism is shown in 'B', and 'C' shows the related signal processing hardware.

Force curves are the plots of the force on a cantilever tip as a function of the distance between the tip and the sample. To plot the force curve, a voltage signal in the form of a triangular wave is applied to the z piezo (for movement of the piezo in vertical direction). The sample whose properties are to be determined is mounted on the piezo. The signal causes the piezo to undergo a number of cycles of expansion and contraction and, thus, the sample approaches and withdraws from the tip repeatedly. When the sample approaches the tip, the cantilever remains undeflected until the tip and the sample are close enough to interact. Figure 2 shows a typical force curve.

Force curves for indentation studies, unlike AFM imaging, require exact measurement of cantilever and sample positions, as the accuracy in determination of these displacements would influence other measurements obtained from the force curves. Sample movement is through the piezo whose exact response to applied

†For correspondence.

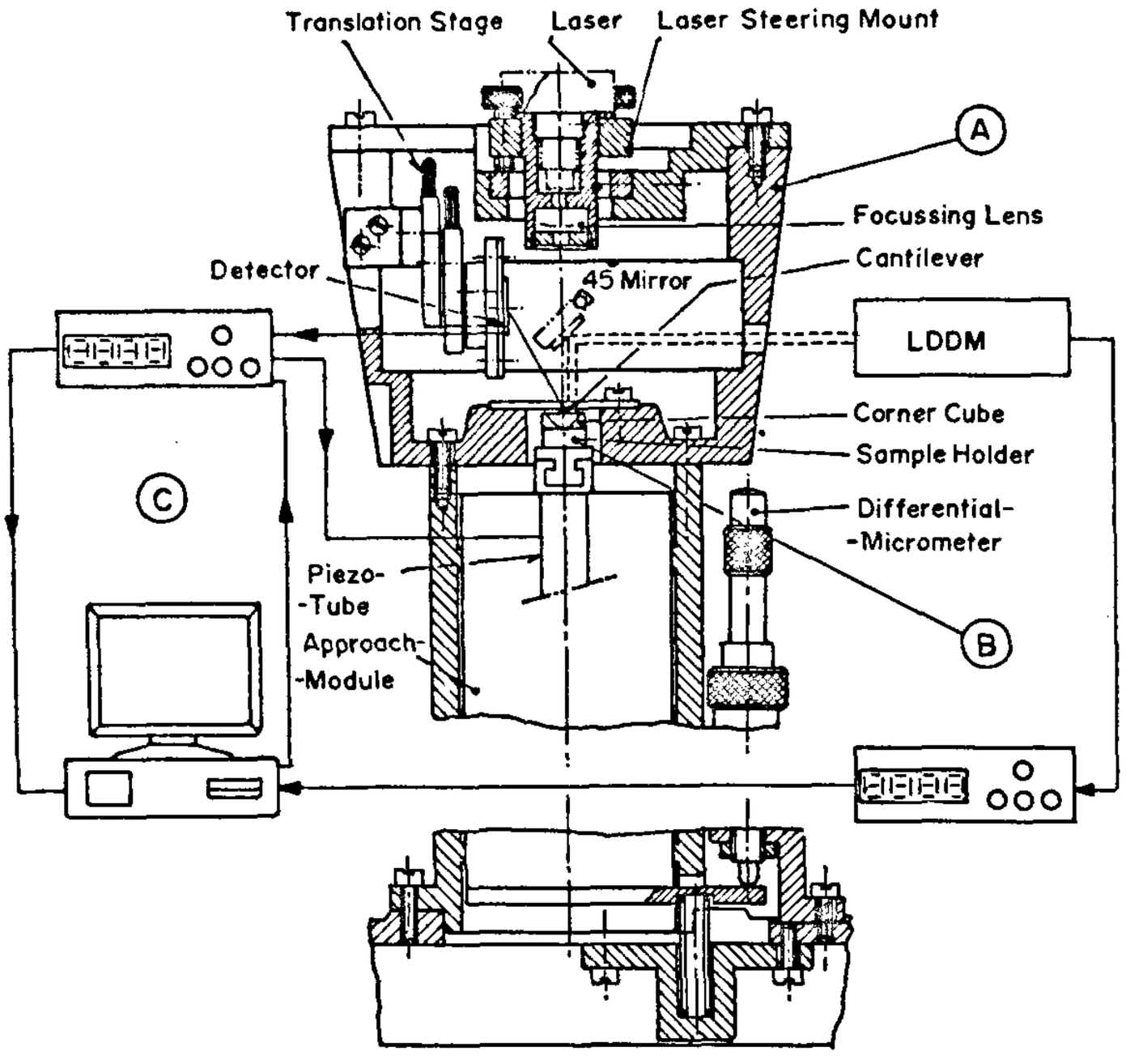

Figure 1. Instrumental details showing AFM integrated with LDDM.

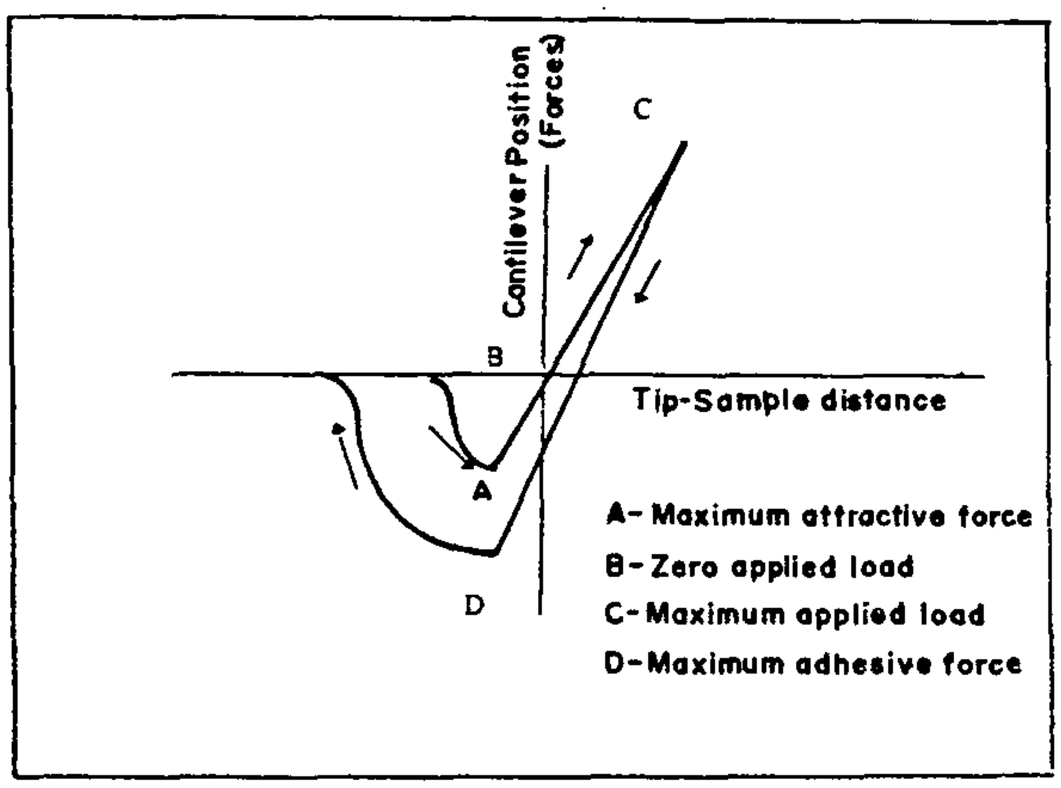

Figure 2. Typical AFM curve.

voltage is required for determining the properties of the sample.

The piezo actuator used in this study was a radially polarized PZT tube with an outer diameter of 12.7 mm, length of 68 mm, and wall thickness of 0.7 mm. The change in length of the tube actuator can be calculated[7] from the following equation:

$$\Delta L = (L/W)\, d_{31} \cdot V,$$

where L is the length of the piezo tube, W is the wall thickness, d_{31} is the piezoelectric strain coefficient and V is the applied voltage. Using the manufacturer's value of -173×10^{-12} m/V for d_{31}, the computed sensitivity is 16.6 nm/V, whereas the measured value from the force curve (Figure 3 *a*), taking linear behaviour is 24 nm/V. This is 47% higher than the calculated value. This is quite in order, as it has been observed by other authors[5] as well.

In situ measurements of displacement of this tube were carried out by placing a corner cube and introducing a mirror at 45° as shown Figure 1. Laser beam from the LDDM was targeted on the corner cube and the reflected beam was aligned to the phase detector in LDDM. AFM and LDDM were interfaced with the computer through their respective controllers.

The expansion and contraction of the piezo tube was controlled by the use of an appropriate computer software. Voltage in the form of triangular waveform was applied to the piezo with the help of DAC card DT-2821 (Data Translation Marlborn, MA). Doppler shift of the laser frequency caused by displacement of the piezo tube was detected by the phase detector, as the frequency of the reflected beam is proportional to the

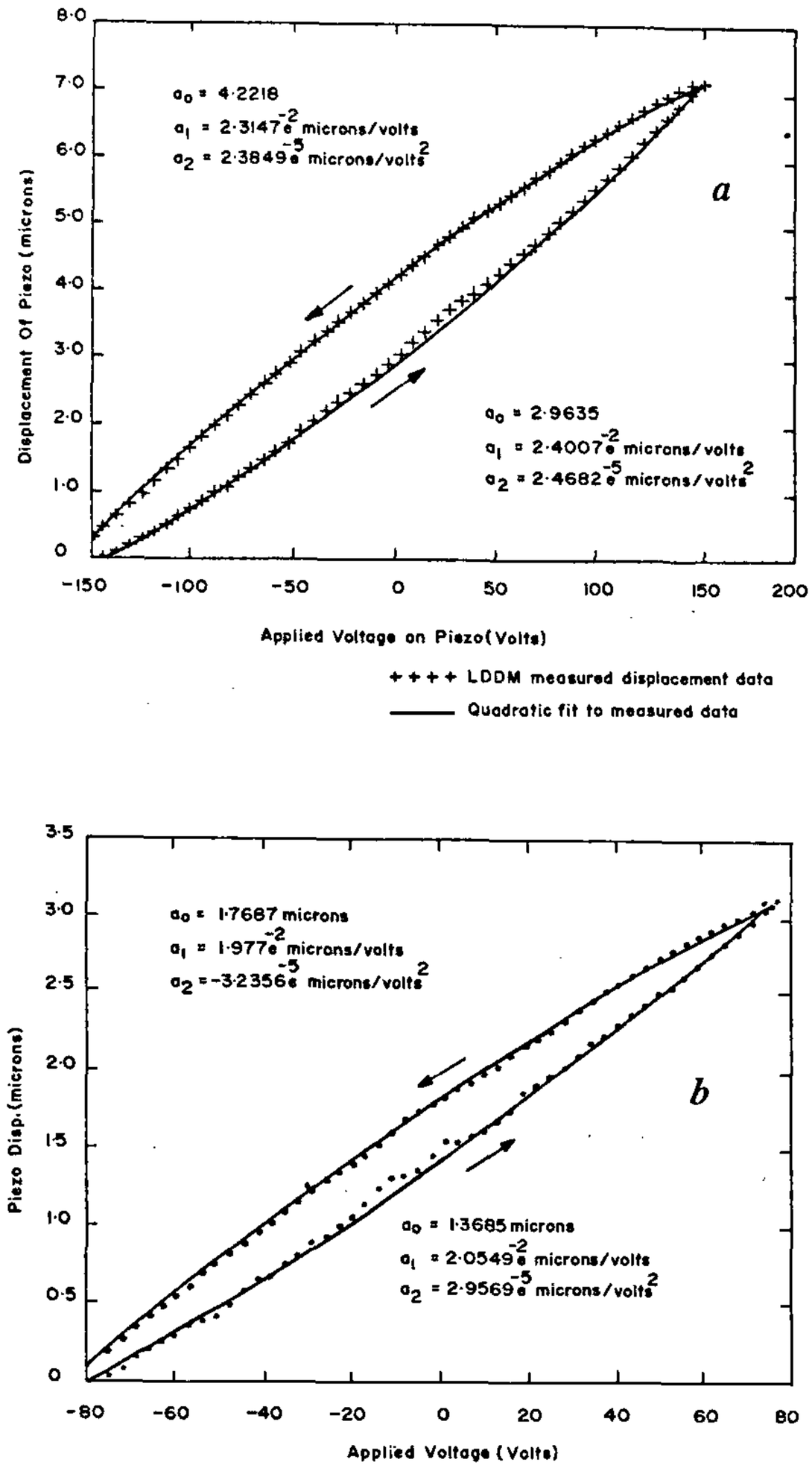

Figure 3 *a* and *b*. Actuator response as a function of applied voltage.

displacement. Digitized detector output was connected to the computer through RS-232-C port. Two sets of experiments were carried out. In the first set, the piezo tube was moved to its full range i.e. from –150 V to +150 V and back to –150 V. In the second set, voltage range of –75 V to +75 V was used. The waveform was applied through a DT card, whose voltage range was –10 V to +10 V. The voltage range was divided into 100 equal steps, the steps of 81 DAC units (0.4 V) for the full range and 40 DAC units (0.2 V) for the half range. Thus, the displacement of the actuator was studied over the specified voltage range which is required for matching sample loading through the same piezo expansion rate. Triangular waveform used for the movement of the piezo tube had a time period of 26.6 s. This is significant, as this time period matches with the pixel–pixel delay period, while acquiring the force curve data.

This data was used to evaluate a second-order polynomial, $D = a_0 + a_1V + a_2V^2$, wherein a_0, a_1, a_2 are constants, D is the displacement and V the applied voltage. Two separate polynomials were obtained from Figure 3 *a*, *b*, one for the expansion and the other for the contraction, which describe the response of the actuator accurately. Each polynomial was used separately while studying the loading–unloading of sample through expansion–contraction of the piezo actuator.

Determination of cantilever displacement (obtained with optical deflection technique)[8] requires accurate calibration of PSD. Detector voltage to distance relationship is determined by the movement of detector stage micrometer and recording the change in PSD output voltage. This calibration has been used to convert the measured detector response to distance. The detector response was measured to be 1.2 mV/μ, the length of the cantilever was 85 microns and the distance between the cantilever and detector was 32 mm.

Alternatively, the detector calibration can be done from the initial part of the loading curve, when the sample just comes in contact with the cantilever. At this point, the movement of the cantilever can be considered as the movement of the sample itself.

HOPG, silicone elastomer, mica and GaAs samples were taken for this study. HOPG and mica were prepared by exfoliation in air. GaAs was cleaned with hydrofloric acid. All measurements were performed in a glove box, containing dry nitrogen. The glove box was thermally insulated.

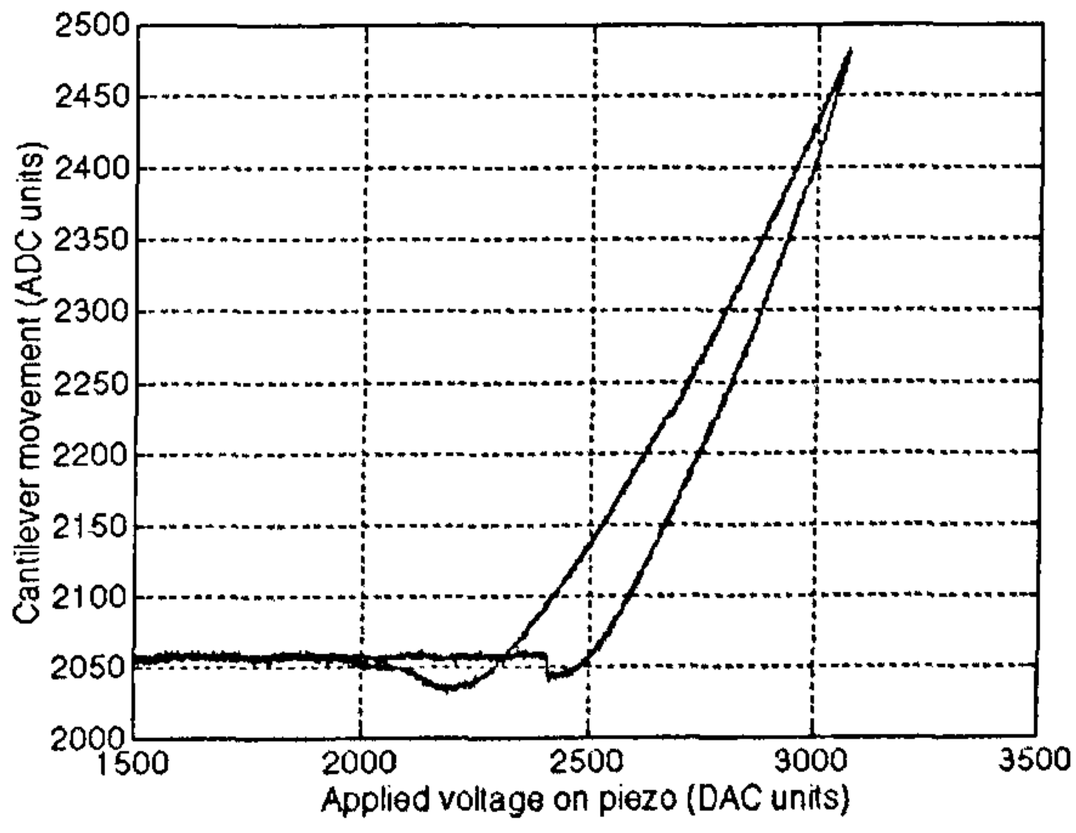

Figure 4. A typical plot of cantilever movement as a function of applied voltage on actuator.

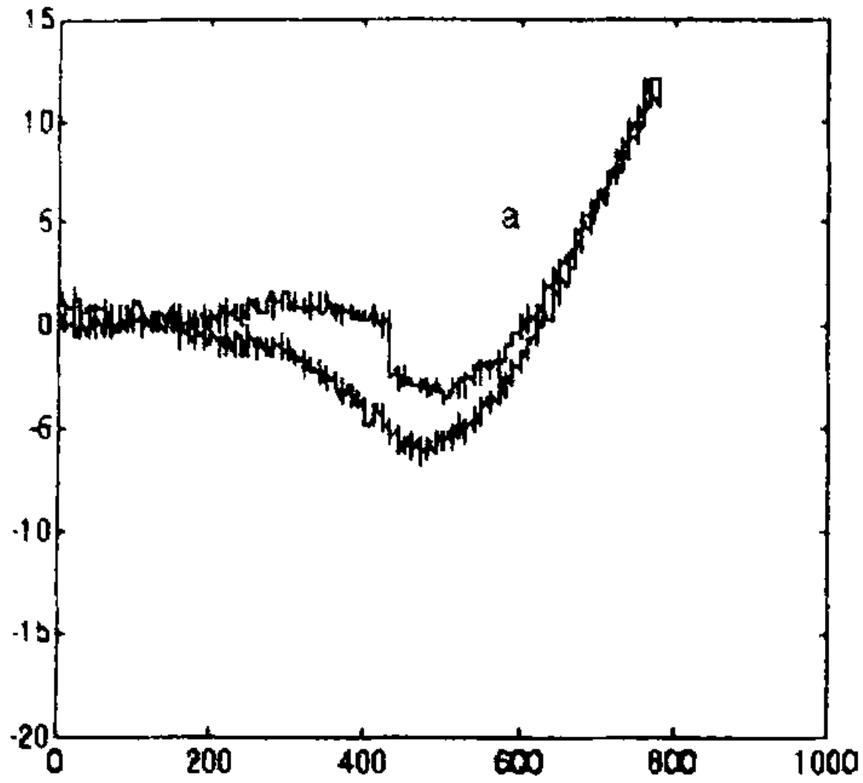

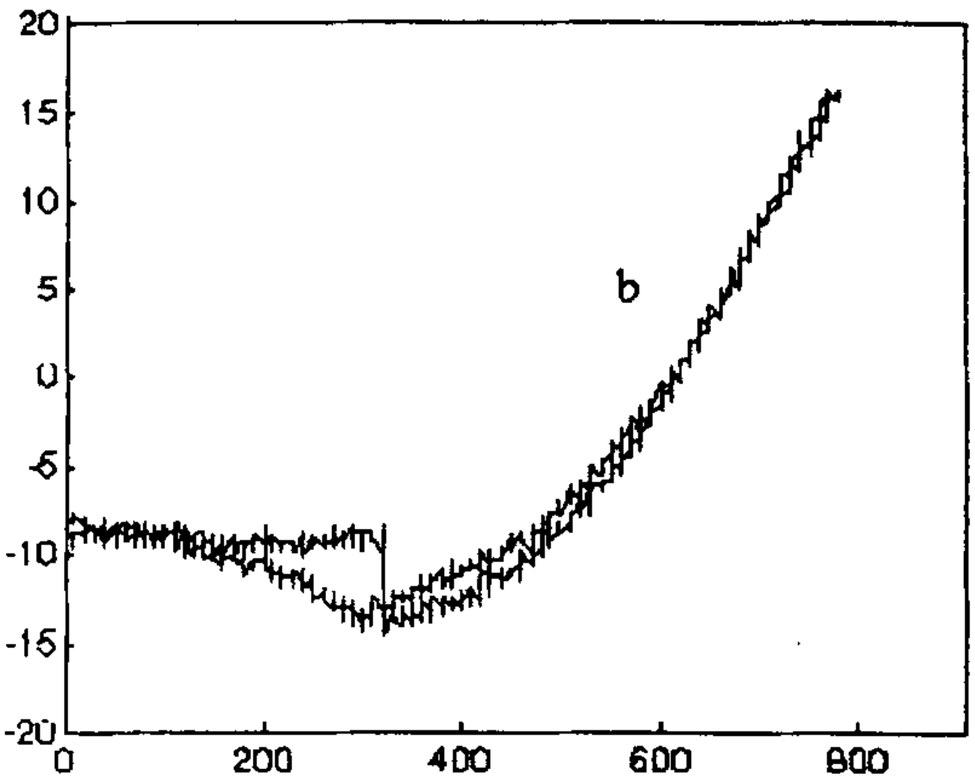

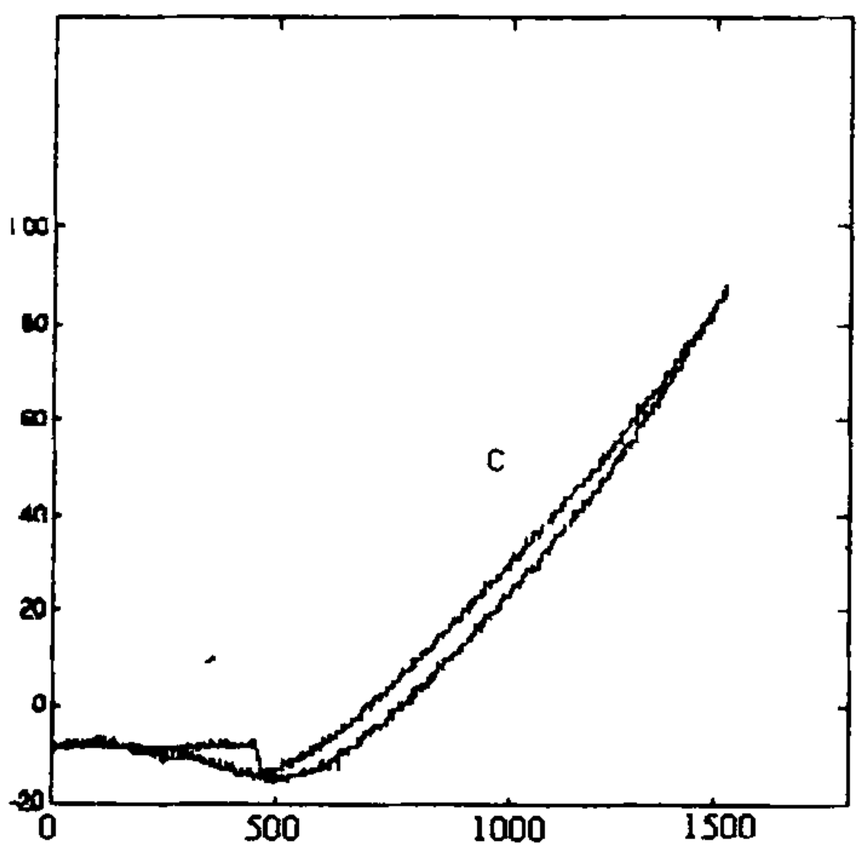

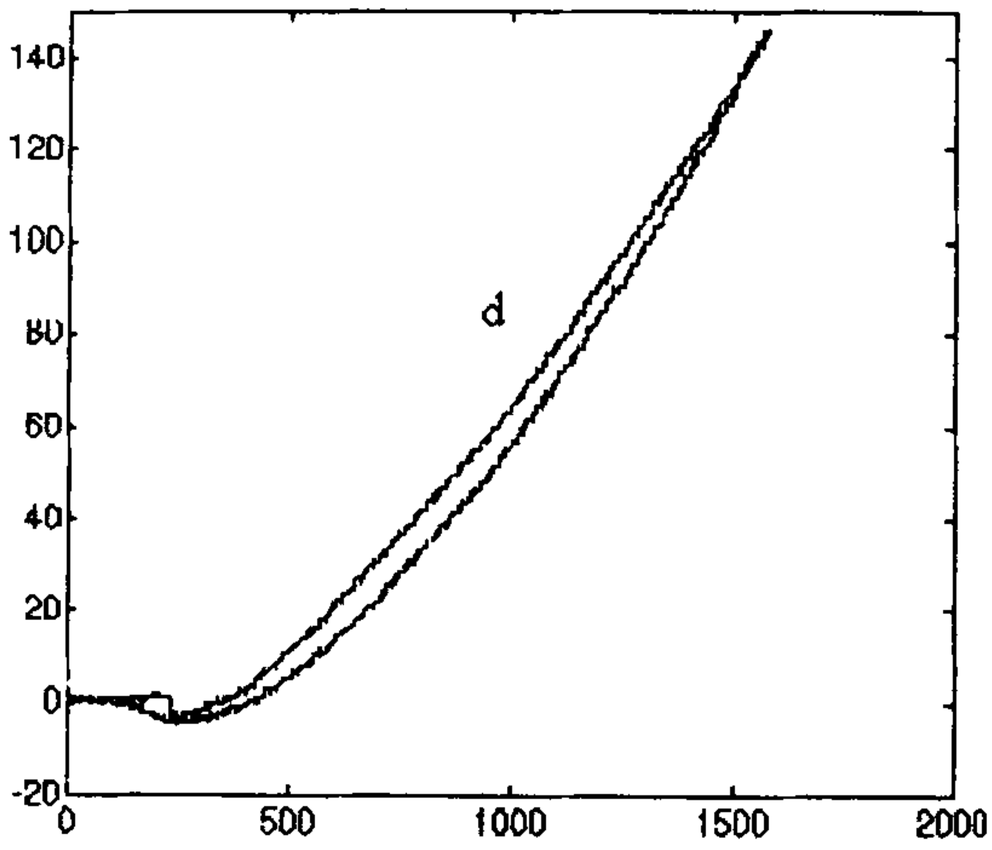

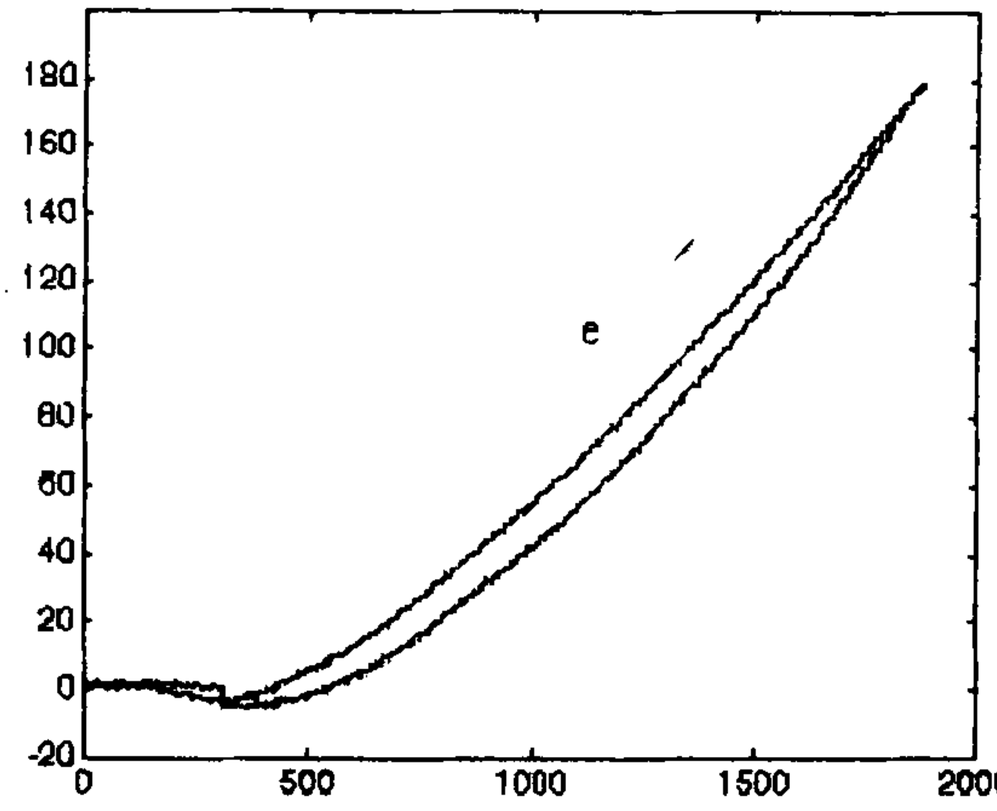

Figure 5. The corrected force curves for various loads, without reverse path effect for silicone elastomer.

The piezo tube carrying the sample was moved in z direction in ranges over which it was calibrated, as described earlier. The force curve data was obtained by giving a triangular wave voltage with minimum DAC step (12 bit resolution) to the sample actuator.

For measuring the cantilever movement, PSD output was taken through ADC channel with a gain of 8 and 4 (range of ± 1.25 V and ± 2.5 V, respectively). For every increment in the DAC step, the corresponding cantilever movement in the form of ADC data was stored and displayed (Figure 4). From the stored data, the force curves at different loads for silicone elastomer were plotted (Figure 5), using linear detector calibration and piezo calibration polynomials. Two different polynomials were used for loading and unloading of the sample. These curves are free from reverse path effect.

Nanoscale indentation hardness of hydrogenated carbon thin films have been studied by Web and Komvopoulos[9] using atomic force and point contact microscopy. AFM images obtained with silicon nitride tips of nominal radius less than 20 nm demonstrated that carbon films possess very similar topographies and root mean square values in the range of 0.7–1.1 nm. Nanoindentation and wear experiments performed with diamond tips of radius equal to about 20 nm revealed a significant enhancement of the hardness and wear resistance with necessary film thickness.

The capability of AFM to quantitatively measure the nanomechanical properties of metals via nanoindentation using lead magnesium niobate (PMN) crystals instead of PZT have been illustrated using three single crystal of chromium, molybdenum, and tungsten by Hues *et al.*[10].

The HFM is being used to study a variety of phenomena including adhesion, tribology, and the mechanical properties of surfaces on the nanometer scale. As a result, the technique is evolving from a qualitative imaging tool to a quantitative probe. There is a serious problem associated with severe hysteresis and creep of PZT actuators used in these instruments, which limits their performance in quantitative applications. We have solved this problem by measuring *in situ* PZT actuator displacement independently by LDDM to correct the force curves, as detailed earlier.

Indentation parameters, load and penetration depth, are determined from the force curves plotted earlier (Figure 5 *a–e*). Here, the cantilever tip acts as an indenter and penetrates the sample as it is loaded. The depth of penetration has been obtained by subtracting cantilever movement from the sample movement in the loading range of the force curve. Tip load deforms sample according to its elastic or plastic behaviour depending upon the mechanical properties.

The deformation of the tip while studying the samples e.g. mica, HOPG, GaAs and silicone elastomers is negligible since the reported hardness of silicon tip material is much higher than the samples. Further, the loads applied while studying the samples are low and result in stresses well within their elastic limits.

Figure 6 shows that silicone elastomer behaves almost ideally. Load increases linearly with penetration depth

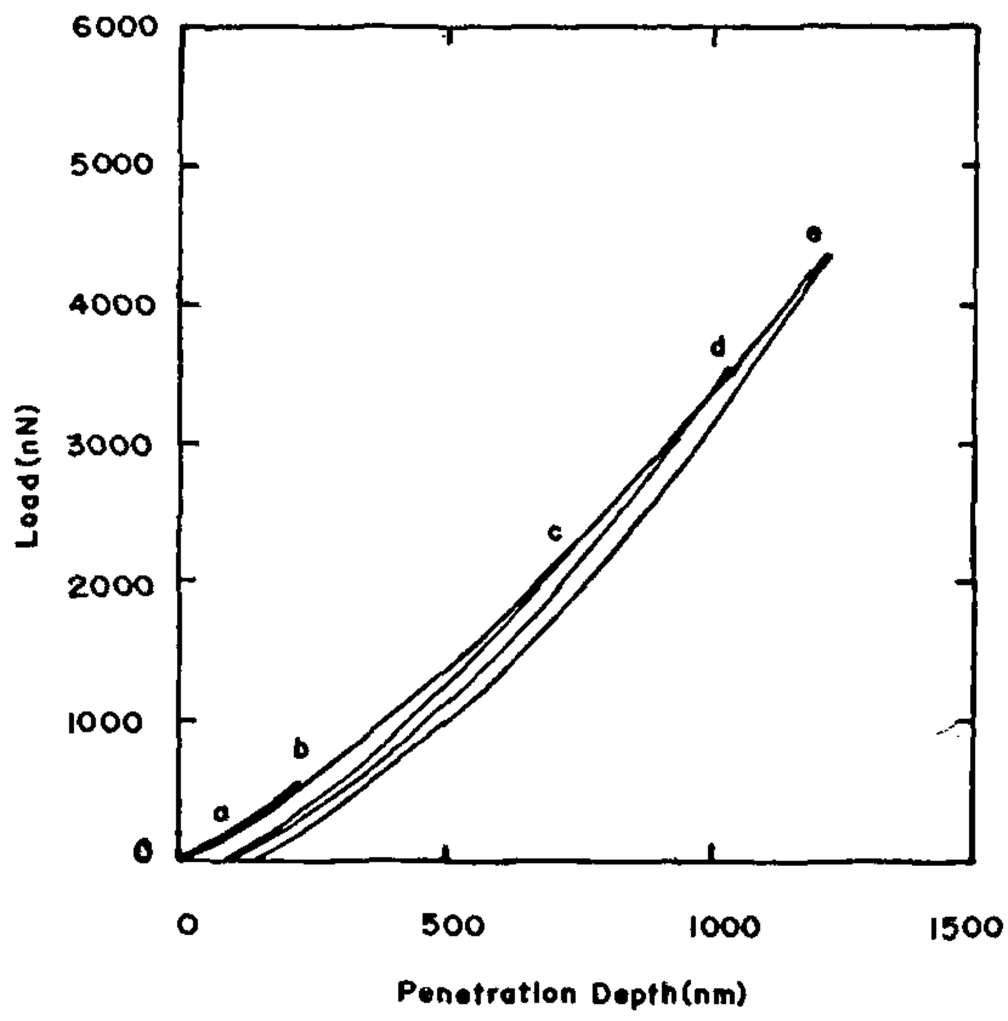

Figure 6. Penetration depth as a function of applied load for silicone elastomer.

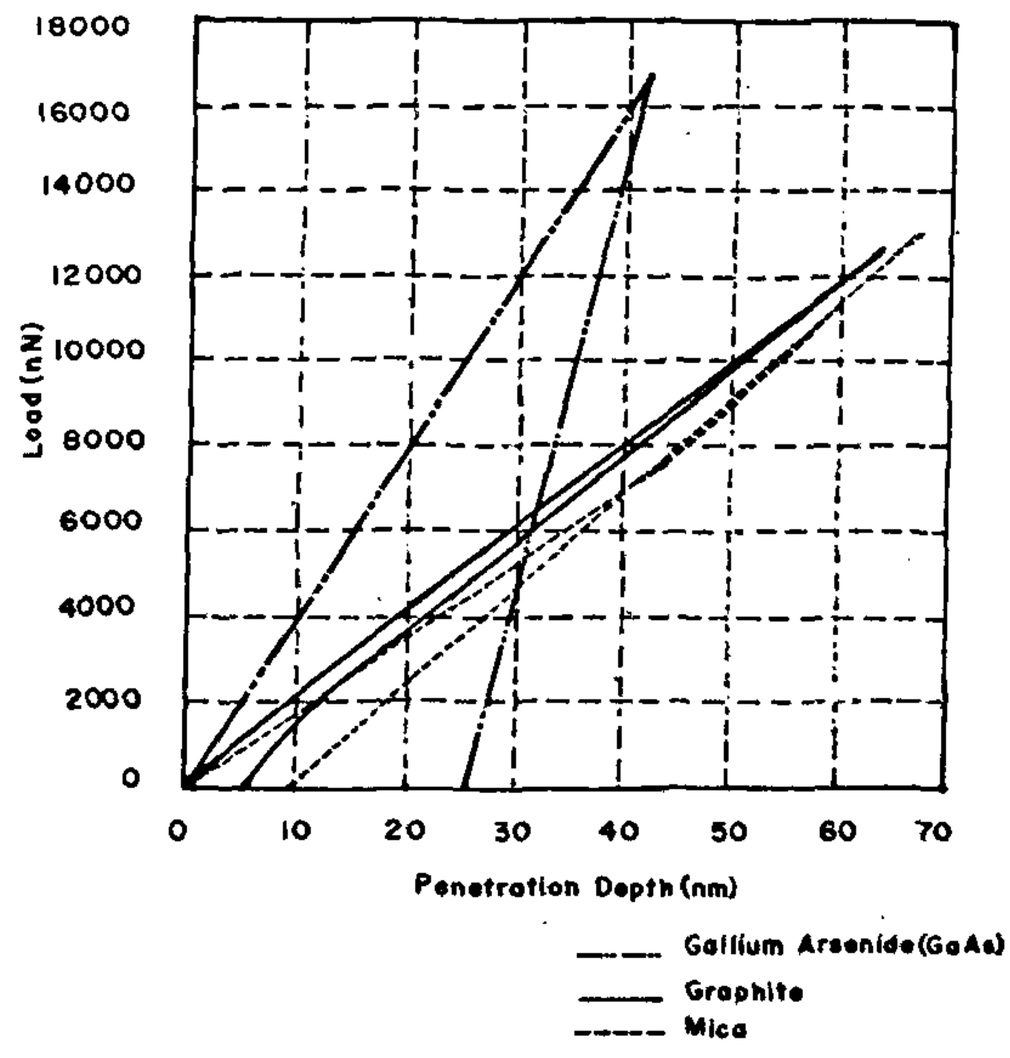

Figure 7. The load penetration depth plots for mica, HOPG and GaAs.

up to a load of 500 nN. For a load of 0.5 μN, the penetration depth is 220 nm. After this load, the sample deforms plastically leaving behind residual depth at zero load. This, however, increases with the applied load. For a maximum load of 4.4 μN, the penetration depth is 1200 nm. Each plot is based on an average of five readings of penetration depth at each point wherein the variation did not exceed 5%.

For mica, HOPG and GaAs, the load vs penetration depth results are shown in Figure 7.

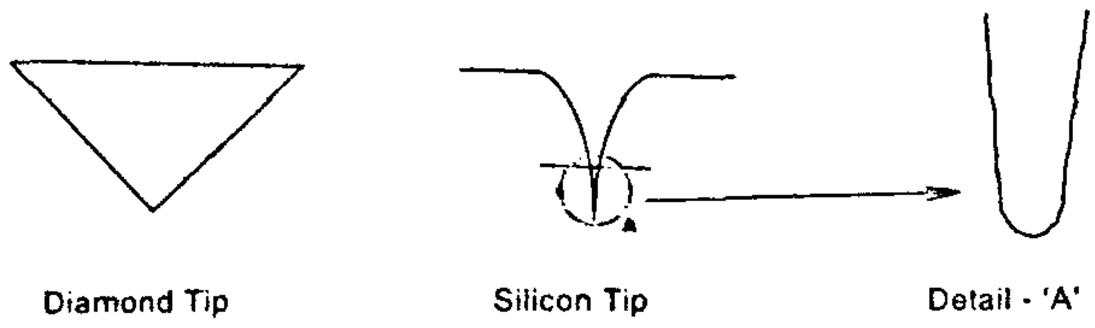

Figure 8. Geometry of silicon and diamond tips integrated with AFM cantilevers.

Table 1. Load (F), penetration depth (h) and computed and bulk volumes of the modulus of electricity (E) in the elastic range

Material	F	h	E (Computed)	E^{12} (Bulk)
Silicone elastomer	500	220	90.6 MPa	15–25 MPa
Mica	4500	40	5.6 GPa	15–20 GPa
Graphite (HOPG)	12000	59	10.1 GPa	5–25 GPa
GaAs	16150	45	17.8 GPa	70–90 GPa

The indentation plots show that the variation of load with penetration depth can be taken nearly linear for the loads in the elastic range of the materials. The relation between load (F) and penetration depth given by Snedden[11], is:

$F = 2\,E\,r\,h/(1-\mu^2)$ (for cylindrical flat ended indenter),

wherein E is Young's modulus of elasticity, r is radius of contact area (taken as tip radius), h is penetration depth, and μ is Poisson's ratio.

It is not necessary to have an accurate value of μ to get a reasonable value of E.

The silicon tips used in this study have much higher aspect ratio compared to diamond tips. The shape of silicon tip penetrating into the sample approximates a cylinder (Figure 8) and as such it is safe to use the above relationship.

Referring to Figure 6 (for silicone elastomer) and Figure 7 (for mica, HOPG and GaAs) for load vs penetration depth, the values of Young's moduli for these materials can be computed using Snedden's relationship.

In the elastic range, the values of load (F) and penetration depth (h), and the computed values of E have been listed in Table 1. In computing the values of E, a value of r equal to 9 nm is used. The values of μ used are 0.48 for silicone elastomer and 0.33 for the other materials.

AFM indentor tip may encounter layers of contamination and oxide layers which may have significant effect on mechanical properties; it may be a convolution of the properties of all the layers in contact with the tip. Actual dimensions of the tip and cantilever (which are taken from the commercial data) may be different from the values used. Hence the E (computed) values and E (bulk) reported in the literature differ widely.

1. Binnig, G., Quate, C. F. and Gerber, Ch., *Phys. Rev. Lett.*, 1986, **56**, 930–933.
2. Kaul, A. D., Singh, N., Sonkusare, A., Kumar, P. and Wadhwa, S. S., *Curr. Sci.*, 1997, **73**, 738–743.
3. Bonnel, D. A. (ed.), *Scanning Tunneling Microscopy and Spectroscopy Theory, Techniques and Applications*, VCH, New York, 1993, pp. 191–249.
4. Burnham, N. A. and Colton, R. J., *J. Vac. Sci. Tech.*, 1989, **A7**, 2906–2913.
5. Hues, S. M., Draper, C. F., Lee, K. P. and Colton, R. J., *Rev. Sci. Inst.*, 1994, **65**, 1561–1565.
6. Product catalogue of M/S Optodyne, 1180 Mahalo Place, Compton, CA 90220, USA, 1990, pp. 9–13.
7. Technical Addition to Bulletin 66011/F, Vernitron Limited, England S09 5QF, 1988, pp. 1–2.
8. Meyer, G. and Amer, N. M., *App. Phys. Lett.*, 1988, **53**, 2400–2405.
9. Web, B. and Komvopoulos, K., *Trans. ASME*, 1995, **117**, 594–601.
10. Hues, S. M., Draper, C. F. and Colton, R. J., *J. Vac. Sci. Technol.*, 1994, **B12**, 2211–2214.
11. Sneddon, I. N., *Int. J. Eng. Sci.*, 1965, **3**, 47.
12. a. Mental, C. L., *Engineering Materials Handbook*, McGraw Hill; b, Alfred, J., *et al.*, *The Practising Scientists' Handbook*, Von Nostrand.

ACKNOWLEDGEMENTS. We thank all the members of STM/AFM group in CSIO, particularly Mr Narinder Singh, Mr Anil Sonkusare, Mr Pradeep Kumar, Ms Jasjit Kaur and Mr Vijay Mohal for experimental and technical support.

Received 16 November 1998; revised accepted 26 March 1999

Langmuir–Blodgett films of poly alkyl thiophenes: Preparation and characterization of multilayers

N. Somanathan*, A. Dhathathreyan and G. Wegner†

Chemical Sciences Division, Central Leather Research Institute, Adyar, Chennai 600 020, India
†Max Planck Institut fur Polymer Forschung, Ackermannweg 10, D55128 Mainz, FRG

The interfacial behaviour of poly alkyl thiophene monolayers formed at air/water interface have been studied using π-A isotherms. These formed stable condensed monolayers on water and could be transferred by the Langmuir–Blodgett (LB) technique. The UV visible spectra of the LB films showed that the polythiophenes form well-defined aggregates with their long axes nearly vertical to the layer plane. Optical microscopy in the Brewster angle set-up showed rigid striated structures in the case of hexyl-substituted polymer while the cyclohexyl derivative showed a less oriented monolayer. In the case of hexyl-substituted polymer (LB) films, the planar polythiophene main chains lie roughly edge-on parallel to the substrate while side chains are approximately orthogonal to the substrate.

IN the last two decades, increasing demand for new polymers has been evidenced in the area of functional materials, designed for specific applications often in the electronic and communication technologies system[1].

*For correspondence. (e-mail: nsomanathan@hotmail.com)